Cell Metabolism
Article

Rim2α Determines Docking and Priming States in Insulin Granule Exocytosis

Takao Yasuda,[1] Tadao Shibasaki,[1] Kohtaro Minami,[1] Harumi Takahashi,[1] Akira Mizoguchi,[3] Yoshitsugu Uriu,[4] Tomohiro Numata,[4] Yasuo Mori,[4] Jun-ichi Miyazaki,[5] Takashi Miki,[1,6] and Susumu Seino[1,2,7,*]
[1]Division of Cellular and Molecular Medicine, Department of Physiology and Cell Biology
[2]Division of Diabetes and Endocrinology, Department of Internal Medicine
Kobe University Graduate School of Medicine, Kobe, Hyogo 650-0017, Japan
[3]Department of Neural Regeneration and Cell Communication, Mie University Graduate School of Medicine, Tsu, Mie 514-8507, Japan
[4]Department of Synthetic Chemistry and Biological Chemistry, Graduate School of Engineering, Kyoto University, Kyoto 615-8510, Japan
[5]Division of Stem Cell Regulation Research, Osaka University Graduate School of Medicine, Suita, Osaka 565-0871, Japan
[6]Department of Autonomic Physiology, Graduate School of Medicine, Chiba University, Chuo-ku, Chiba 260-8670, Japan
[7]Core Research for Evolutional Science and Technology (CREST), Japan Science and Technology Agency, Kawaguchi, Saitama 332-0012, Japan
*Correspondence: seino@med.kobe-u.ac.jp
DOI 10.1016/j.cmet.2010.05.017

SUMMARY

Insulin secretion is essential for maintenance of glucose homeostasis, but the mechanism of insulin granule exocytosis, the final step of insulin secretion, is largely unknown. Here, we investigated the role of Rim2α in insulin granule exocytosis, including the docking, priming, and fusion steps. We found that interaction of Rim2α and Rab3A is required for docking, which is considered a brake on fusion events, and that docking is necessary for K^+-induced exocytosis, but not for glucose-induced exocytosis. Furthermore, we found that dissociation of the Rim2α/Munc13-1 complex by glucose stimulation activates Syntaxin1 by Munc13-1, indicating that Rim2α primes insulin granules for fusion. Thus, Rim2α determines docking and priming states in insulin granule exocytosis depending on its interacting partner, Rab3A or Munc13-1, respectively. Because *Rim2α*$^{-/-}$ mice exhibit impaired secretion of various hormones stored as dense-core granules, including glucose-dependent insulinotropic polypeptide, growth hormone, and epinephrine, Rim2α plays a critical role in exocytosis of these dense-core granules.

INTRODUCTION

Stimulus-secretion coupling has been characterized in neurons and neuroendocrine and endocrine cells (Burgoyne and Morgan, 2003; Sudhof, 2004; Seino and Shibasaki, 2005). Pancreatic β cells, in which insulin is stored as dense-core granules, play a central role in glucose homeostasis. Although understanding of the molecular mechanisms of cell signaling in insulin secretion has deepened remarkably in recent years, the mechanisms of insulin granule exocytosis, the final step in the insulin secretory process, are largely unknown.

Recently, various molecules interacting with the insulin granules have been identified (Brunner et al., 2007), including Rab27A (Kasai et al., 2005), granuphilin (Gomi et al., 2005), ZnT8 (Nicolson et al., 2009), Noc2 (Matsumoto et al., 2004), collectrin (Fukui et al., 2005), and Rap1 (Shibasaki et al., 2007). Mutation of the Rab27A gene was discovered from Griscelli syndrome in human, characterized by hypopigmentation and loss of cytotoxic killing activity by cytotoxic T lymphocytes (Ménasché et al., 2000). The same mutation found in the mouse coat-color mutant *ashen* causes a defect in insulin granule exocytosis (Kasai et al., 2005). *Granuphilin*$^{-/-}$ mice, *ZnT8*$^{-/-}$ mice, *Noc2*$^{-/-}$ mice, and transgenic mice overexpressing collectrin also exhibit impaired insulin secretion and abnormal glucose homeostasis.

We previously identified Rab3-interacting molecule 2 (Rim2) by yeast two-hybrid screen of a clonal pancreatic β cell (MIN6) cDNA library (Ozaki et al., 2000). Rim2 is now known as a multidomain protein that occurs as three variants, including Rim2α, Rim2β, and Rim2γ (Wang and Südhof, 2003). Rim2α, the full-length form of Rim2, is composed of an N-terminal Zn^{2+}-finger domain, a central PDZ and C_2A domains, and a C-terminal C_2B domain. Rim2β lacks the N-terminal Zn^{2+}-finger domain of Rim2α, whereas Rim2γ is composed only of the C-terminal C_2B domain of Rim2α with flanking sequences. Rim2α interacts with Rab3A (Ozaki et al., 2000), Munc13-1 (Dulubova et al., 2005), and Rab8 (Fukuda, 2003) at the N-terminal region. In addition to interaction with these proteins, Rim2α binds to cAMP-GEFII (also referred to as Epac2) (Ozaki et al., 2000; Shibasaki et al., 2004) and ELKS (Ohara-Imaizumi et al., 2005; Inoue et al., 2006) through the central PDZ domain, to Piccolo through a C_2A domain (Fujimoto et al., 2002), to RIM-BPs through a PXXP sequence between the two C_2 domains (Hibino et al., 2002), and to Liprin-α1 and synaptotagmin 1 through the C-terminal C_2B domain (Schoch et al., 2002). These findings suggest that Rim2α functions as a scaffold protein and that it is involved in regulated exocytosis. Indeed, Rim2α has been found to be involved in cAMP-potentiated insulin secretion through the Epac2 pathway in in vitro studies (Ozaki et al., 2000; Kashima et al., 2001). Although Rim2α is

expressed mainly in endocrine and neuroendocrine cells such as pancreatic β cells, pituitary, and adrenal gland, it is unknown how Rim2α acts in the steps in the process of exocytosis, including recruitment, docking, priming, and fusion.

Rim1α, an isoform of Rim2α, is expressed mainly in brain and a putative Rab3 effector involved in the regulation of synaptic vesicle fusion (Wang et al., 1997). Studies of *Rim1α*$^{-/-}$ mice (Castillo et al., 2002; Lonart et al., 2003) and the null mutation of Rim in *C. elegans* (Koushika et al., 2001) indicate that Rim1α is important for long-term potentiation by increasing neurotransmitter release at mossy fiber synapses in the CA3 region in hippocampus of cerebrum and that it is involved in a postdocking step. To clarify the role of Rim2α in endocrine function both in vitro and in vivo, we generated *Rim2α*$^{-/-}$ mice. In the course of our study, Schoch et al. also generated *Rim2α*$^{-/-}$ mice and reported the phenotype of the mice (Schoch et al., 2006). They found no apparent developmental abnormalities of these mice, but there were slight behavioral differences and slightly lower survival rates compared to *Rim2α*$^{+/+}$ mice. They also found no changes in body fat content or blood glucose levels in *Rim2α*$^{-/-}$ mice. However, no study of endocrine or neuroendocrine functions in *Rim2α*$^{-/-}$ mice was reported.

In the present study, we show that Rim2α is required for the docking and priming states in insulin granule exocytosis through interaction with Rab3A and Munc13-1, respectively, and that, although docking is necessary for K^+-induced exocytosis, it is unnecessary for glucose-induced exocytosis. In addition, we found secretory defects in various hormones, including glucose-dependent insulinotropic polypeptide (GIP), growth hormone (GH), and epinephrine in *Rim2α*$^{-/-}$ mice in vivo. Thus, Rim2α is a key molecule in insulin granule exocytosis and also is required in normal secretion of hormones associated with glucose homeostasis.

RESULTS

Insulin and GIP Secretion Are Impaired in *Rim2α*$^{-/-}$ Mice In Vivo

The Rim2 gene has three independent promoters that create three variant forms of Rim2, Rim2α, Rim2β, and Rim2γ (Wang and Südhof, 2003) (Figure S1A available online). We found that, among the three variants, Rim2α is predominantly expressed in pancreatic islets and insulin-secreting MIN6 cells (Figure S1B and S1C). We generated *Rim2α*$^{-/-}$ mice in which the fourth exon of the Rim2 gene was replaced by Neo cassette (Figure S1D). The absence of Rim2α expression in *Rim2α*$^{-/-}$ mice was confirmed by northern blot analysis, reverse transcription PCR, and immunoblot analysis (Figures S1E–S1G). The expression levels of Rim2β and Rim2γ were not changed in *Rim2α*$^{-/-}$ mice (Figure S1H). *Rim2α*$^{-/-}$ mice were viable and fertile. *Rim2α*$^{-/-}$ mice exhibited islet hyperplasia (*Rim2α*$^{+/+}$ = 7,887.6 ± 728.1 μm^2; *Rim2α*$^{-/-}$ = 15,620.4 ± 1,486.7 μm^2; n = 4 and 100 islets; $p < 0.01$) and a relatively increased number of α cells (*Rim2α*$^{+/+}$ = 14.7% ± 1.5% of islets; *Rim2α*$^{-/-}$ = 40.0% ± 2.5% of islets; $p < 0.01$; n = 3, n = 53 for *Rim2α*$^{+/+}$ and n = 37 for *Rim2α*$^{-/-}$) (Figure S1I).

We performed intraperitoneal glucose tolerance test (IPGTT) to examine pancreatic endocrine function in *Rim2α*$^{-/-}$ mice. The fasting blood glucose levels of *Rim2α*$^{-/-}$ mice were significantly decreased compared those of *Rim2α*$^{+/+}$ mice (*Rim2α*$^{+/+}$ = 119 ± 3.1 mg/dl; *Rim2α*$^{-/-}$ = 87 ± 4.7 mg/dl; $p < 0.01$; n = 19 for *Rim2α*$^{+/+}$ and n = 17 for *Rim2α*$^{-/-}$). The blood glucose levels of *Rim2α*$^{-/-}$ mice 60 min after intraperitoneal glucose administration were significantly higher than those of *Rim2α*$^{+/+}$ mice. The insulin response during IPGTT in *Rim2α*$^{-/-}$ mice was markedly lower than that in *Rim2α*$^{+/+}$ mice (Figure 1A). We also examined changes in blood glucose and insulin levels after oral glucose administration (OGTT). The blood glucose levels of *Rim2α*$^{-/-}$ mice during OGTT were significantly higher than those of *Rim2α*$^{+/+}$ mice at all time points examined. The insulin levels were markedly reduced in *Rim2α*$^{-/-}$ mice compared to those in *Rim2α*$^{+/+}$ mice (Figure 1B). Similar results were obtained by oral mixed meal administration (Figure 1C). These results suggest that incretin secretion is decreased in *Rim2α*$^{-/-}$ mice. GIP, an incretin secreted by enteroendocrine cells in response to ingestion of nutrients, potentiates glucose-induced insulin secretion (Drucker, 2006). To investigate the possible involvement of incretins in this reduced insulin secretion, we attempted to measure the serum levels of GIP and glucagon-like peptide-1 (GLP-1) in *Rim2α*$^{-/-}$ mice. Although GIP-secreting K cells were present in *Rim2α*$^{-/-}$ mice (Figure S1J), serum GIP levels in *Rim2α*$^{-/-}$ mice were below the sensitivity of assay (Figure 1D). However, the measurement of GLP-1, another incretin, in mouse serum was not possible by using commercially available kits despite several attempts. These results indicate that both insulin and GIP secretion in *Rim2α*$^{-/-}$ mice are markedly impaired.

Insulin Secretion Is Impaired in Pancreatic Islets of *Rim2α*$^{-/-}$ Mice

As shown in Figure 2A, insulin content of the islets of *Rim2α*$^{-/-}$ mice was increased 1.4-fold, compared to that of *Rim2α*$^{+/+}$ mice. Both glucose-induced and Ca^{2+}-triggered insulin secretion (assessed by 60 mM K^+ stimulation) from pancreatic islets of *Rim2α*$^{-/-}$ mice were significantly decreased, compared to those from pancreatic islets of *Rim2α*$^{+/+}$ mice (Figure 2B). We then examined insulin secretion potentiated by cAMP in pancreatic islets of *Rim2α*$^{-/-}$ mice. GIP-potentiated insulin secretion from pancreatic islets of *Rim2α*$^{-/-}$ mice was significantly lower than that of *Rim2α*$^{+/+}$ mice (Figure 2C). The cAMP analog 8-Bromo-cAMP-potentiated insulin secretion also was significantly reduced in pancreatic islets of *Rim2α*$^{-/-}$ mice. These results strongly suggest that Rim2α plays a major role in insulin secretion.

The Number of Docked Insulin Granules Is Decreased in Pancreatic β Cells of *Rim2α*$^{-/-}$ Mice

We investigated the role of Rim2α in insulin granule exocytosis. For this purpose, we analyzed the dynamics of insulin granules in living pancreatic β cells using total internal reflection fluorescence microscopy (TIRFM) (Shibasaki et al., 2007). We confirmed that the modes of insulin granule exocytosis can be classified into three groups depending on the dynamics of the insulin granules: (1) fusion events involving granules that are predocked to the plasma membrane (*old face*); (2) fusion events involving granules that are newly recruited and immediately fused to the plasma membrane without docking (*restless newcomer*); and (3) fusion events involving granules that are

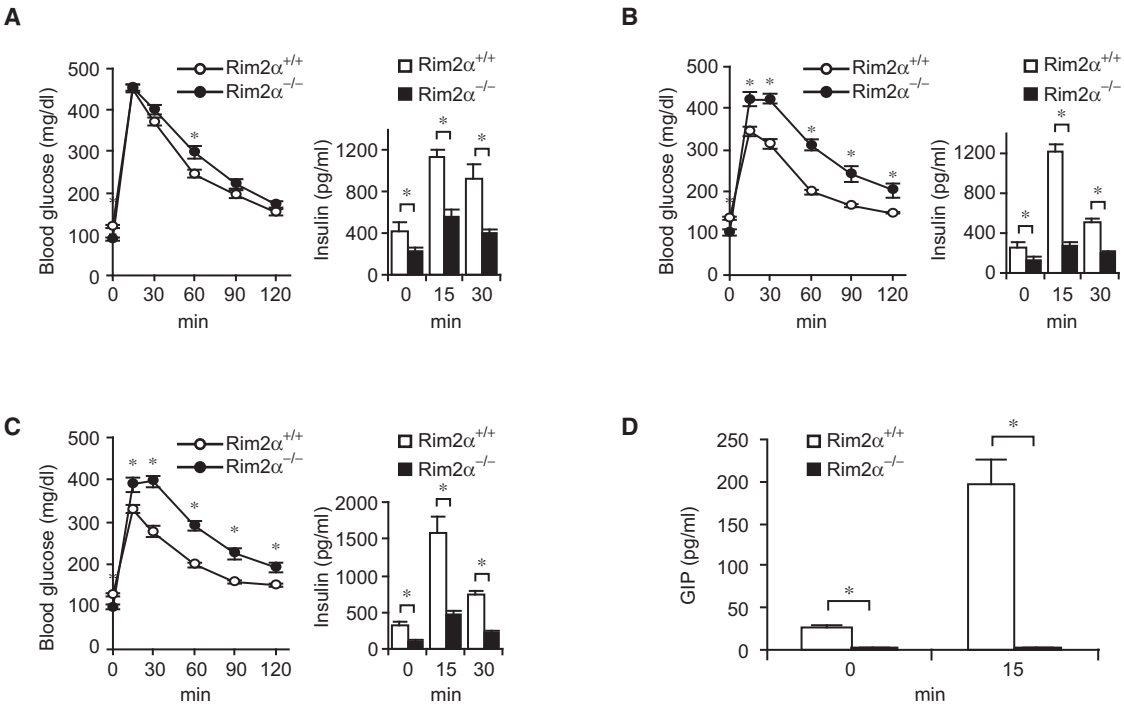

Figure 1. Impaired Insulin and GIP Secretion in *Rim2α*$^{-/-}$ Mice

(A) Changes in blood glucose levels (left) and serum insulin levels (right) after intraperitoneal glucose load in *Rim2α*$^{+/+}$ mice (white) and *Rim2α*$^{-/-}$ mice (black).
(B) Changes in blood glucose levels (left) and serum insulin levels (right) after oral glucose load in *Rim2α*$^{+/+}$ mice (white) and *Rim2α*$^{-/-}$ mice (black).
(C) Changes in blood glucose levels (left) and serum insulin levels (right) after mixed meal load in *Rim2α*$^{+/+}$ mice (white) and *Rim2α*$^{-/-}$ mice (black).
(D) GIP secretion after mixed meal load in *Rim2α*$^{+/+}$ mice (white) and *Rim2α*$^{-/-}$ mice (black).
Data were obtained from three independent experiments (n = 5–19) and expressed as means ± SEM. *p < 0.01 (Student's unpaired t test).
See also Figure S1.

newly recruited, docked, and then fused to the plasma membrane (*resting newcomer*).

As shown in Figure 3A, the number of docked insulin granules in pancreatic β cells of *Rim2α*$^{-/-}$ mice was markedly decreased, compared to that in pancreatic β cells of *Rim2α*$^{+/+}$ mice. We have previously shown that most K^+-induced fusion events involve *old face* (Shibasaki et al., 2007). As expected, the number of fusion events caused by K^+ stimulation in pancreatic β cells of *Rim2α*$^{-/-}$ mice was significantly decreased due to the marked reduction in the number of *old face* (Figure 3B). In contrast, glucose-induced fusion events comprised mainly *restless newcomer*. Fusion events, mainly in the first phase, were markedly decreased in pancreatic β cells of *Rim2α*$^{-/-}$ mice, and those in the second phase were also decreased (Figure 3C). *Resting newcomer*, which docks to the plasma membrane before fusion, were not detected in pancreatic β cells of *Rim2α*$^{-/-}$ mice. These results indicate that Rim2α is required in normal regulation of insulin granule exocytosis.

The Defect in Insulin Granule Exocytosis in *Rim2α*$^{-/-}$ Mice Is Not Due to Changes in Expression or Distribution of Exocytosis-Associated Proteins

We intended to examine the expression and subcellular localization of exocytosis-associated proteins as a consequence of Rim2α deficiency, using pancreatic β cells of *Rim2α*$^{-/-}$ mice. However, the limited number of isolated pancreatic β cells of these mice made such an experiment impossible. We therefore established clonal pancreatic β cells lacking Rim2α (*Rim2α*$^{ko/ko}$ β cells) by crossbreeding *Rim2α*$^{-/-}$ mice and *IT6* mice expressing simian virus 40 large T antigen under human insulin promoter (Miyazaki et al., 1990). The absence of Rim2α expression in Rim2α$^{ko/ko}$ β cells was confirmed by immunocytochemical and immunoblot analyses using anti-Rim2 antibody (Figures 4A and 4B).

To determine whether deficiency of Rim2α affects the expression levels and localization of exocytosis-associated proteins, we compared those of the proteins in MIN6 cells and *Rim2α*$^{ko/ko}$ β cells. We found no significant differences in the expression levels of any of the proteins examined (Figure 4B). The expression levels did not differ in *Rim2α*$^{ko/ko}$ β cells expressing wild-type (WT) Rim2α by adenovirus-mediated gene transfer. We examined localization of Rim2α and exocytosis-associated proteins in MIN6 cells by immunostaining and subcellular fractionation experiments. Rim2α was localized on both insulin granules and plasma membrane (Figures 4A and 4C), whereas Rab3A, Munc13-1, and Syntaxin1 were localized on the plasma membrane (Figure 4C). The localizations of these proteins were the same in *Rim2α*$^{ko/ko}$ β cells.

We then examined insulin secretion in *Rim2α*$^{ko/ko}$ β cells. Both glucose- and K^+-induced insulin secretion from *Rim2α*$^{ko/ko}$ β cells were significantly reduced, compared to those from MIN6 cells (Figure 4D). Similarly to the pancreatic β cells of

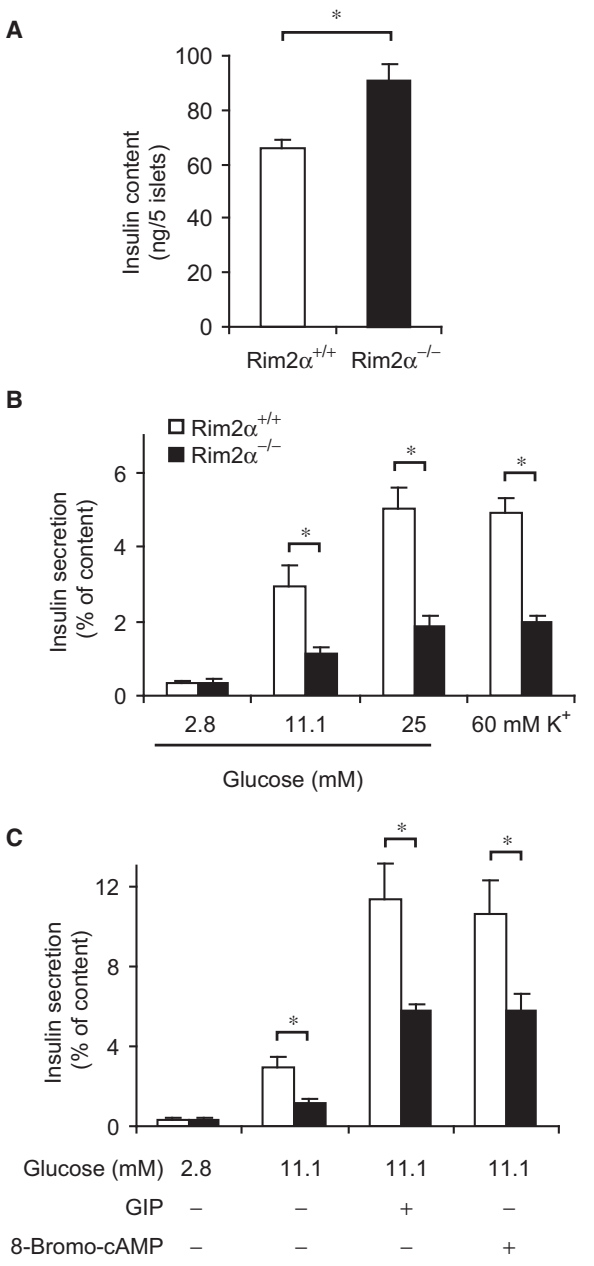

Figure 2. Impaired Insulin Secretion in Pancreatic Islets of *Rim2α*$^{-/-}$ Mice

(A) Insulin contents in pancreatic islets of *Rim2α*$^{+/+}$ mice (white) and *Rim2α*$^{-/-}$ mice (black).

(B) Insulin secretion in response to glucose and 60 mM K^+ in pancreatic islets of *Rim2α*$^{+/+}$ mice (white) and *Rim2α*$^{-/-}$ mice (black).

(C) Effects of cAMP-increasing agents on insulin secretion in pancreatic islets of *Rim2α*$^{+/+}$ mice (white) and *Rim2α*$^{-/-}$ mice (black).

Data were obtained from two to three independent experiments (n = 5–9) and expressed as means ± SEM. *p < 0.01 (Student's unpaired t test).

Rim2α$^{-/-}$ mice, the number of docked insulin granules was significantly decreased in *Rim2α*$^{ko/ko}$ β cells (Figure 4E). Importantly, the defects in both insulin secretion and the number of docked insulin granules were rescued when WT Rim2α was exogenously introduced by adenovirus-based gene transfer (Figures 4D and 4E). These results indicate that Rim2α is required for the docking step in insulin granule exocytosis.

Rim2α, Rab3A, and Munc13-1 Form a Complex Regulated by Glucose

Because the expression levels and localization of exocytosis-associated proteins in *Rim2α*$^{ko/ko}$ β cells did not differ from those in MIN6 cells, we explored the possibility that the interaction of Rim2α and Rim2α-binding proteins is critical for regulated exocytosis of insulin granules. We performed immunoprecipitation experiments on the interaction of Rim2α with Rab3A or Munc13-1 by glucose stimulation. The interaction of Rim2α and Munc13-1 was decreased by glucose stimulation (Figures 4F and S2). However, no interaction of Rim2α and endogenous Rab3A was detected (Figure 4F). This suggests that most of the endogenous Rab3A is likely to be in the GDP-inactivated state because Rim2α binds to the GTP-activated form of Rab3A (Ozaki et al., 2000). In fact, we found that Rim2α interacted with the GTP-activated form of Rab3A (Figure 4F). Therefore, we examined the effect of the active form of Rab3A on the interaction of Rim2α and Munc13-1. The interaction of Rim2α and Munc13-1 in the presence of the constitutively active form of Rab3A (Q81L) (Brondyk et al., 1993) was detected in a glucose concentration-independent manner (Figures 4F and S2). These results indicate that Munc13-1 dissociates from the Rim2α/Munc13-1 complex by glucose stimulation.

Rim2α Is Critical for Docking and Priming of Insulin Granules

The finding of differences in the interactions with these three molecules indicates that Rim2α is involved in the recruitment, docking, and/or priming steps. Rab3A and Munc13-1 have been shown to interact with the N-terminal region of Rim2α (Dulubova et al., 2005). To determine whether the impaired insulin secretion in *Rim2α*$^{ko/ko}$ β cells is caused by defective interaction of Rim2α with Rab3A, Munc13-1, or both of them, we prepared a double mutant (E36A/R37S) of Rim2α that cannot bind to Rab3A but can bind to Munc13-1 (Fukuda, 2004). Using this mutant, we examined insulin secretion and the number of docked insulin granules in *Rim2α*$^{ko/ko}$ β cells. Although the mutant Rim2α (E36A/R37S) was able to restore both glucose- and K^+-induced insulin secretion (Figures 5A, top-left, and 6A), the mutant Rim2α (E36A/R37S) was unable to restore the number of docked insulin granules (Figure 5A, top-right), suggesting that the interaction of Rim2α and Rab3A is required for docking of the insulin granules, but not for fusion of the granules to the plasma membrane. Of interest, because K^+-induced insulin secretion in *Rim2α*$^{ko/ko}$ β cells was significantly higher than that by WT Rim2α gene transfer, the interaction of Rim2α and Rab3A may negatively regulate insulin secretion (Figures 5A, top and lower-left, and 6A), that is, docking may be a state-preventing fusion (i.e., a braking state).

We then prepared a double mutant (K136E/K138E) of Rim2α that cannot bind to Munc13-1 but can bind to Rab3A (Dulubova et al., 2005). Although the mutant Rim2α (K136E/K138E) was unable to restore either glucose- or K^+-induced insulin secretion (Figures 5A, top-left, and 6A), the mutant was able to restore the number of docked insulin granules (Figure 5A, top-right). These

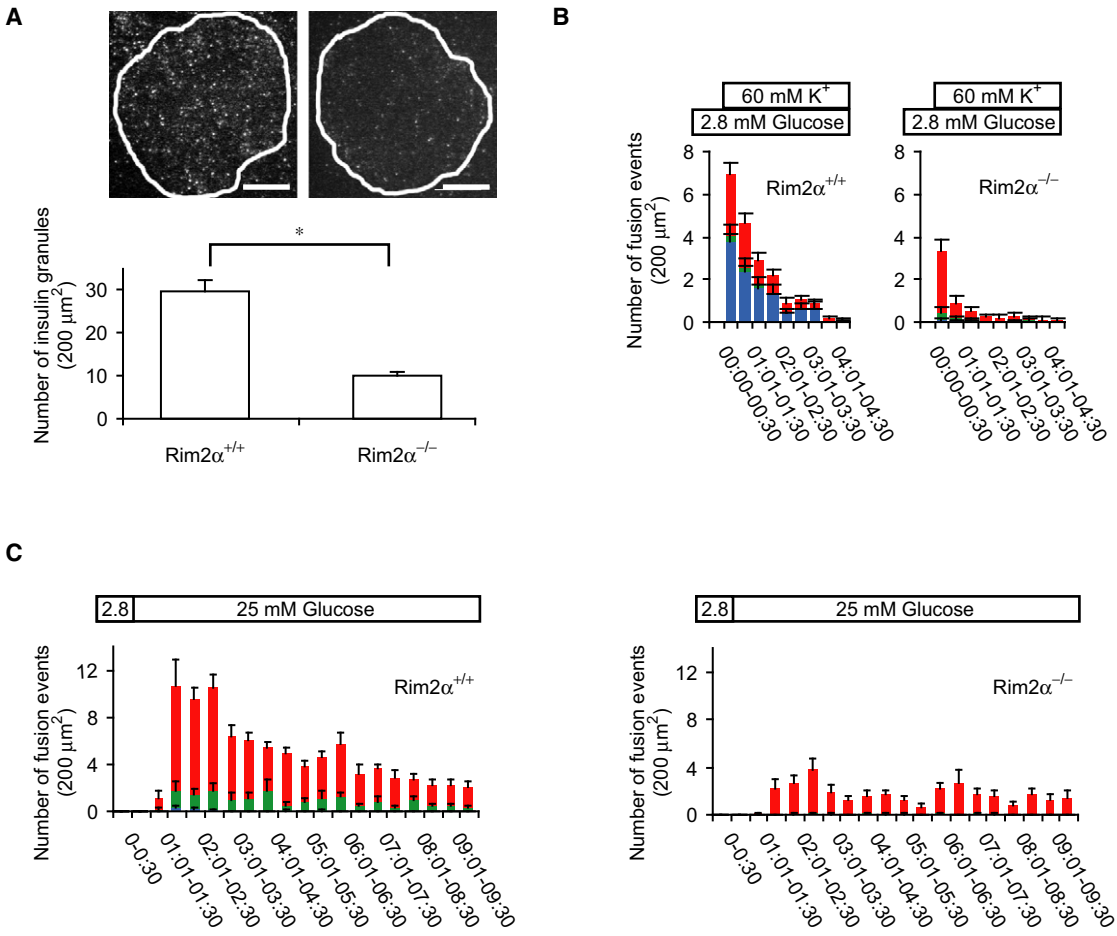

Figure 3. Rim2α-Mediated Insulin Granule Exocytosis

(A) Comparison of the number of insulin granules docked to the plasma membrane in pancreatic β cells of *Rim2α*$^{+/+}$ and *Rim2α*$^{-/-}$ mice. Primary cultured pancreatic β cells were preincubated with HEPES-KRB buffer containing 2.8 mM glucose at 37°C for 30 min, fixed, immunostained with anti-insulin antibody, and observed by TIRFM. The surrounding lines represent the outline of a cell attached to the cover glass. The number of docked granules was measured in a cell surface area of 200 μm^2. Scale bar, 10 μm. Data were obtained from three independent experiments (n = 8) and expressed as means ± SEM. *p < 0.01 (Student's unpaired t test).

(B) Histogram of fusion events at 30 s intervals in pancreatic β cells of *Rim2α*$^{+/+}$ (left) and *Rim2α*$^{-/-}$ (right) mice stimulated with 60 mM K$^+$ in a cell surface area of 200 μm^2. Primary cultured pancreatic β cells were preincubated with HEPES-KRB buffer containing 2.8 mM glucose at 37°C for 30 min. Thirty seconds after acquisition of the image, the primary cultured cells were stimulated with 60 mM K$^+$; 2.8 indicates 2.8 mM glucose. *Old face* (blue): Granules that are predocked to the plasma membrane and fused to the membrane by stimulation. *Restless newcomer* (red): Granules that are newly recruited and immediately fused to the plasma membrane by stimulation. *Resting newcomer* (green): Granules that are newly recruited, docked, and fused to the plasma membrane by stimulation. Data were obtained from five to six independent experiments (n = 6–7) and expressed as means ± SEM.

(C) Histogram of fusion events in pancreatic β cells of *Rim2α*$^{+/+}$ (left) and *Rim2α*$^{-/-}$ (right) mice stimulated with 25 mM glucose in a cell surface area of 200 μm^2. Fusion events were analyzed as shown in (B). Data were obtained from five to six independent experiments (n = 6–7) and expressed as means ± SEM.

results suggest that interaction of Rim2α and Munc13-1 after the docking step is required for insulin granule exocytosis (Figures 5A, top and lower-right, and 6A).

To examine whether Rim2α enhances Munc13-1 activity in pancreatic β cells, we evaluated insulin secretion in *Rim2α*$^{ko/ko}$ β cells by phorbol 12-myristate 13-acetate (PMA), which is known to enhance Munc13-1 activity in pancreatic β cells (Betz et al., 1998; Kang et al., 2006). Glucose-induced insulin secretion was restored in Rim2α$^{ko/ko}$ β cells in the presence of PMA (Figures 5B, left, and 6B). However, the number of docked insulin granules was not increased in *Rim2α*$^{ko/ko}$ β cells (Figure 5B, middle). These results suggest that Rim2α directly activates Munc13-1 and that it regulates postdocking steps of insulin granule exocytosis (Figure 5B, right).

Activation of Munc13-1 is proposed to change Syntaxin1 from the closed state to the open state, initiating the priming step of granule exocytosis (Madison et al., 2005). Thus, Syntaxin1 might not be activated in *Rim2α*$^{ko/ko}$ β cells. If that is the case, introduction of exogenous open Syntaxin1 into *Rim2α*$^{ko/ko}$ β cells should bypass the interaction of Rim2α and Munc13-1 to stimulate insulin secretion directly. To investigate this possibility, we examined insulin secretion and the number of docked insulin granules in *Rim2α*$^{ko/ko}$ β cells after gene transfer of open Syntaxin1 (Dulubova et al., 1999). Open Syntaxin1 fully restored

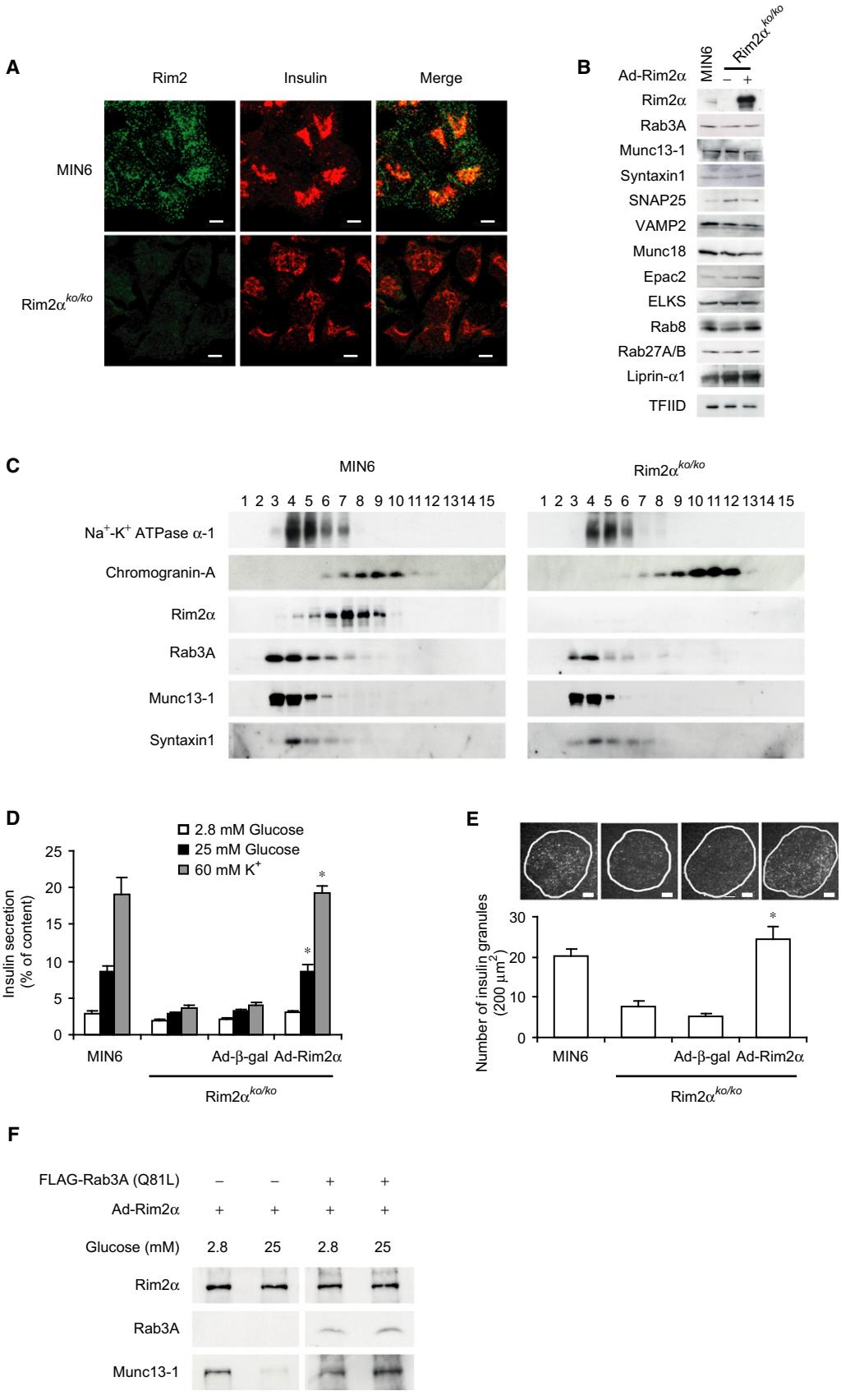
A
Rim2
Insulin
Merge
MIN6
Rim2α ko/ko
B
MIN6
Rim2α ko/ko
Ad-Rim2α
– +
Rim2α
Rab3A
Munc13-1
Syntaxin1
SNAP25
VAMP2
Munc18
Epac2
ELKS
Rab8
Rab27A/B
Liprin-α1
TFIID
C
MIN6
Rim2α ko/ko
1 2 3 4 5 6 7 8 9 10 11 12 13 14 15
Na+-K+ ATPase α-1
Chromogranin-A
Rim2α
Rab3A
Munc13-1
Syntaxin1
D
2.8 mM Glucose
25 mM Glucose
60 mM K+
Insulin secretion (% of content)
25
20
15
10
5
0
MIN6
Ad-β-gal
Ad-Rim2α
Rim2α ko/ko
E
Number of insulin granules (200 μm2)
30
20
10
0
MIN6
Ad-β-gal
Ad-Rim2α
Rim2α ko/ko
F
FLAG-Rab3A (Q81L) – – + +
Ad-Rim2α + + + +
Glucose (mM) 2.8 25 2.8 25
Rim2α
Rab3A
Munc13-1

both glucose- and K^+-induced insulin secretion, but WT Syntaxin1 did not restore it (Figures 5C, left, and 6C). In contrast, both forms of Syntaxin1 were unable to restore the number of docked insulin granules (Figure 5C, middle). These findings indicate that interaction of Rim2α and Munc13-1 is required in the process of exocytosis between the docking and fusion steps, suggesting that such interaction underlies priming of insulin granules.

Rim2α Is Required for Epac2-Potentiated Insulin Secretion

Rim2α was originally identified as a molecule that interacts with Epac2 (Ozaki et al., 2000). Because Epac2 is responsible for cAMP-dependent, PKA-independent exocytosis, interaction of Rim2α and Epac2 is thought to be involved in cAMP-potentiated insulin secretion (Ozaki et al., 2000; Kashima et al., 2001). To clarify the role of Rim2α in cAMP-potentiated insulin secretion, we utilized *Rim2α*$^{ko/ko}$ β cells, preparing a triple mutant (R682A, L688A, and G689A) (PDZ-AAA) of Rim2α that disrupts the interaction of Rim2α and Epac2 (Shibasaki et al., 2004). This mutant Rim2α (PDZ-AAA) significantly rescued, although not completely, glucose-induced insulin secretion. Importantly, the glucose-induced insulin secretion potentiated by the Epac-specific cAMP analog 8-pCPT-2′-*O*-Me-cAMP-AM (Vliem et al., 2008) failed to potentiate insulin secretion in these cells (Figure 7). These results make clear that Rim2α mediates cAMP-induced, Epac2-dependent insulin secretion.

Rim2α Deficiency Causes Multiple Defects in Hormone Secretion

Systemic analysis of offspring from heterozygous mating revealed that *Rim2α*$^{-/-}$ mice were smaller than littermate Rim2α$^{+/+}$ mice (Figure S1K). Both basal- and hypoglycemia-induced GH secretion were markedly reduced in *Rim2α*$^{-/-}$ mice (Figure S1L), and insulin-like growth factor-1 (IGF-1) levels were decreased in the mice (Figure S1M). In addition, hypoglycemia-induced epinephrine secretion was significantly decreased in *Rim2α*$^{-/-}$ mice (Figure S1N). In contrast, hypoglycemia-induced glucagon secretion was significantly increased in *Rim2α*$^{-/-}$ mice (Figure S1O), a finding consistent with the increase in the number of α cells. Taken together, these results show that Rim2α is required for normal regulation of hormone secretion associated with glucose homeostasis.

DISCUSSION

Rim1α is a multidomain adaptor protein that was discovered as a putative effector of Rab3 (Wang et al., 1997). The null mutation of Rim in *C. elegans* was shown to decrease the number of fusion-competent vesicles, suggesting a role in the postdocking process (Koushika et al., 2001). We previously identified Rim2α as a molecule interacting with Epac2 and found that it was required for cAMP-dependent, PKA-independent insulin secretion in vitro (Ozaki et al., 2000; Kashima et al., 2001). However, the role of Rim2α in exocytosis has not been clarified. To address this issue, we generated *Rim2α*$^{-/-}$ mice. In the course of our study, Schoch et al. reported the phenotype of *Rim2α*$^{-/-}$ mice, which they generated independently, but no changes in blood glucose levels in *Rim2α*$^{-/-}$ mice were found (Schoch et al., 2006). In the present study, we have analyzed the phenotype of *Rim2α*$^{-/-}$ mice in detail both in vivo and in vitro.

We recently reported that K^+-induced exocytosis comprises mainly granules already docked to the plasma membrane (*old face*), whereas glucose-induced exocytosis consists almost exclusively of granules that are newly recruited to the plasma membrane (*restless newcomer*) (Shibasaki et al., 2007). In the present study, we show that a mutant Rim2α (E36A/R37S) that does not bind to Rab3A did not rescue docked granules in *Rim2α*$^{ko/ko}$ β cells but was able to rescue glucose-induced insulin secretion to a degree similar to that rescued by WT Rim2α. This finding indicates that, although docking of insulin granules to the plasma membrane requires interaction of Rim2α and Rab3A, it is not essential for glucose-induced insulin secretion. Indeed, despite the defect in docking, K^+-induced insulin secretion is significantly increased in *granuphilin*$^{-/-}$ mice (Gomi et al., 2005).

It has been thought that the priming and fusion steps occur after the docking step in neuronal cells (Verhage and Sørensen, 2008). The priming step is proposed to be initiated by unfolding of the SNARE protein Syntaxin1 from the closed to the open state, which can bind SNAP25 and VAMP2, which are other SNARE proteins, to form the SNARE complex. The mutant Syntaxin1 (L166A/E167A), which is a constitutively open form (Dulubova et al., 1999), can rescue the fusion of synaptic vesicles in *C. elegans* Syntaxin null mutants (Richmond et al., 2001). Although Munc13-1 is thought to be a priming factor in large dense-core and synaptic vesicles and the interaction of Rim1α and Munc13-1 is thought to regulate priming (Ashery et al., 2000; Betz et al., 2001), the molecular mechanism of the priming

Figure 4. Generation and Characterization of *Rim2α*$^{ko/ko}$ β Cells

(A) Immunocytochemical analysis of MIN6 cells and *Rim2α*$^{ko/ko}$ β cells. Green, Rim2; red, Insulin. Scale bar, 5 μm.

(B) Comparison of expression levels of exocytosis-related proteins among MIN6 cells, *Rim2α*$^{ko/ko}$ β cells, and *Rim2α*$^{ko/ko}$ β cells expressing WT Rim2α.

(C) Subcellular localization of exocytosis-related proteins in *Rim2α*$^{ko/ko}$ β cells. *Rim2α*$^{ko/ko}$ β cells were homogenized, and organelles in the supernatants were separated on discontinuous sucrose gradients. Fractions were subjected to immunoblot analysis with anti-Na^+-K^+-ATPase α-1 (plasma membrane marker), Chromogranin-A (large dense-core granule marker), Rim2, Rab3A, Munc13-1, and Syntaxin1.

(D) Insulin secretion from *Rim2α*$^{ko/ko}$ β cells. Data were obtained from three independent experiments (n = 7–11) and expressed as means ± SEM. *$p < 0.01$ versus corresponding values in Ad-β-gal (Student's unpaired t test).

(E) The number of insulin granules docked to the plasma membrane in *Rim2α*$^{ko/ko}$ β cells. Data were obtained from three independent experiments (n = 11–16) and expressed as means ± SEM. *$p < 0.01$ versus Ad-β-gal (Student's unpaired t test). Scale bars, 5 μm.

(F) Effect of glucose on the interaction of Rim2α and Rab3A or Munc13-1. After *Rim2α*$^{ko/ko}$ β cells expressing c-Myc-tagged WT Rim2α were stimulated with 25 mM glucose for 30 min, their lysates were incubated with lysates of COS-1 cells expressing FLAG-tagged Rab3A (Q81L). Their mixture was subjected to immunoprecipitation with anti-c-Myc antibody-conjugated agarose and then to immunoblot analysis with anti-Rim2, Rab3A, and Munc13-1 antibodies.

See also Figure S2.

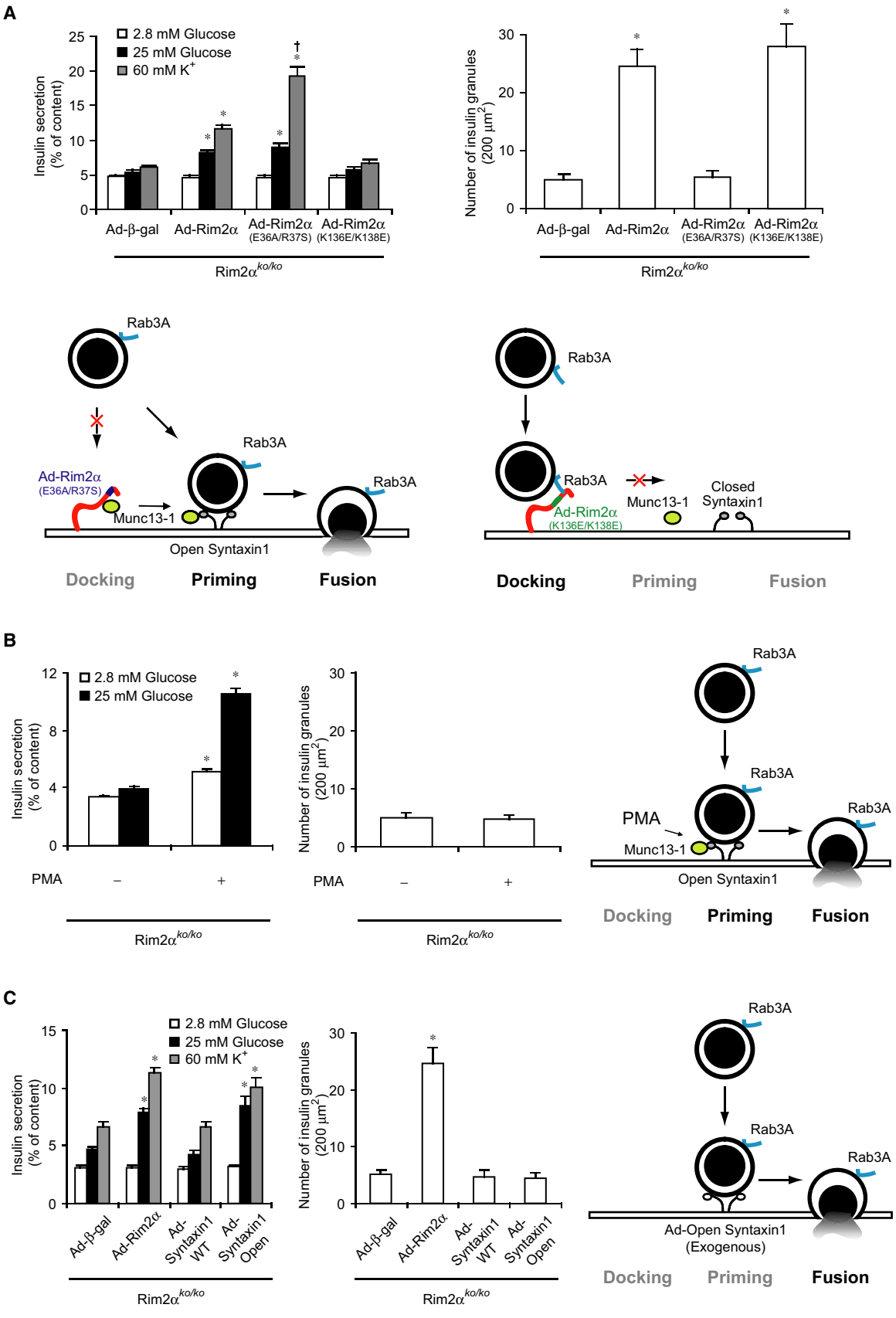
A
2.8 mM Glucose
25 mM Glucose
60 mM K+
Insulin secretion (% of content)
Number of insulin granules (200 μm2)
Ad-β-gal
Ad-Rim2α
Ad-Rim2α (E36A/R37S)
Ad-Rim2α (K136E/K138E)
Rim2α ko/ko
Rab3A
Munc13-1
Open Syntaxin1
Closed Syntaxin1
Docking
Priming
Fusion
B
PMA
Ad-Open Syntaxin1 (Exogenous)
C
Ad-Syntaxin1 WT
Ad-Syntaxin1 Open

step has not been clarified. In *Rim1α*$^{-/-}$ brain, the expression level of Munc13-1 is decreased (Schoch et al., 2002), and Munc13-1 is not enriched at the active zone of mossy fiber terminals of mouse hippocampus (Andrews-Zwilling et al., 2006). We found that both the expression level and the localization of Munc13-1 are not changed in *Rim2α*$^{ko/ko}$ β cells but that Munc13-1 dissociates from the Rim2α/Munc13-1 complex by glucose stimulation and activates Syntaxin1 to evoke fusion. Rim2α is thus a critical molecule in determining both the docking and priming states in accord with its interacting partner Rab3A or Munc13-1, respectively (Figure S3).

We previously showed that Rim2α is involved in cAMP-dependent, PKA-independent insulin secretion through the Epac2 pathway (Ozaki et al., 2000; Kashima et al., 2001). We show here that glucose-induced insulin secretion potentiated by the Epac-specific analog 8-pCPT-2′-*O*-Me-cAMP-AM is not induced in *Rim2α*$^{ko/ko}$ β cells expressing mutant Rim2α (PDZ-AAA). This further confirms that Rim2α is required in the Epac2 pathway for potentiation of insulin secretion by cAMP. Because Epac2 also activates Rap1 by cAMP, which may increase the size of the nondocked granule pool and/or facilitate the recruitment of granules to the plasma membrane (Shibasaki et al., 2007; Seino et al., 2009), both Rim2α and Rap1 act cooperatively in cAMP-induced, Epac2-dependent insulin secretion.

In this study, we also found that Rim2α exerts a suppressive effect on the voltage dependence of inactivation of voltage-dependent Ca^{2+} channel (VDCC) currents and controls the intracellular Ca^{2+} concentration in pancreatic β cells (Figure S4), as was found of Rim1α in neurons (Kiyonaka et al., 2007). Rim2α has been shown to interact with VDCCs directly or indirectly (Hibino et al., 2002; Shibasaki et al., 2004). It is generally accepted that neuronal secretion represents vesicle fusion in response to Ca^{2+} microdomains, which requires close proximity of the vesicles to the sites of focal Ca^{2+} entry (Llinás et al., 1992; Barg et al., 2001; Hoppa et al., 2009). These findings together with the role of Rim2α further suggest the importance of the Ca^{2+} microdomain for insulin granule exocytosis in pancreatic β cells. Rim2α is expressed predominantly in endocrine and neuroendocrine cells (Ozaki et al., 2000). Because we found defects in the secretion of various hormones, including GIP, GH, and epinephrine, all of which are stored as dense-core granules, Rim2α might well play a similar role in exocytosis of these hormones.

EXPERIMENTAL PROCEDURES

Reagents

A full list of reagents is provided in the Supplemental Experimental Procedures.

Generation of *Rim2α*$^{-/-}$ Mice

Rim2α$^{-/-}$ mice were generated by replacing the amino acid coding sequences in exon 4 of mouse Rim2 with Neo cassette as described (Figure S1). Detailed description and genotyping strategy are provided in Supplemental Experimental Procedures.

Generation of Rim2α-Deficient Clonal Pancreatic β Cells

Clonal pancreatic β cells lacking Rim2α (*Rim2α*$^{ko/ko}$ β cells) were established by crossbreeding *Rim2α*$^{-/-}$ mice and *IT6* mice expressing SV40 large T antigen under human insulin promoter that developed highly differentiated β cell tumors (Miyazaki et al., 1990). Twenty-seven lines of Rim2α$^{ko/ko}$ β cells were generated from a 10-week-old mouse lacking Rim2α and carrying a large T antigen load (*Rim2α*$^{-/-}$; *IT6* mouse) as previously described (Shibasaki et al., 2007).

Cell Culture

MIN6 cells, *Rim2α*$^{ko/ko}$ β cells, and COS-1 cells were grown in Dulbecco's modified Eagle's medium (DMEM) containing 10% heat-inactivated fetal bovine serum and maintained in a humidified incubator with 95% air and 5% CO_2 at 37°C.

RNA Extraction and Quantitative RT-PCR

Total RNA from mouse pancreatic islets and β cell lines was isolated using the RNeasy Kit. For reverse transcription, ReverTra Ace-α-Kit was used. Quantitative real-time PCR was carried out by SYBR Premix Ex Taq with the primers for mouse Rim2α (forward 5′-GGAAAATCATCCTGGCTGTC and reverse 5′-ATGTCACTGGCAATCTGGTG), mouse Rim2β (forward 5′-ACGA AGTCCATCAGTGTCCA and reverse 5′-GCTCAGACCATTCCAAATCC), and HPRT (forward 5′-TCTTTGCTGACCTGCTGGATT and reverse 5′-GGCTT TGTATTTGGCTTTTCC) using a model 7000 thermal cycler (Applied Biosystems, Foster City, CA). HPRT was used as internal control (Figure S1).

In Vivo Experiments

Glucose (1.5 g/kg body weight), mixed meal (Twinline: 10 ml/kg body weight), or insulin (0.4 IU/kg body weight) was administered intraperitoneally or orally to overnight (16 hr) fasted male mice at 16–22 weeks of age as described previously (Miki et al., 2005). Blood glucose levels were measured by Antsense III glucose analyzer (Bayer Yakuhin, Osaka, Japan); ELISA system was used for measurement of serum insulin (Morinaga, Tokyo, Japan), GIP and GH (LINCO Research, St. Charles, MO), and IGF-1 (R&D Systems, Minneapolis, MN). Measurements of epinephrine levels were performed by SRL (Tokyo, Japan).

Immunohistological Analysis

The pancreases were removed from *Rim2α*$^{+/+}$ and *Rim2α*$^{-/-}$ mice and were immersion fixed in 4% paraformaldehyde in 0.1 M phosphate buffer (pH 7.4). Fixed tissues were dehydrated and embedded in paraffin by conventional procedure. Five-micrometer-thick paraffin sections were stained with guinea pig anti-insulin antibody and mouse anti-glucagon antibody, followed by Alexa Fluor 546-conjugated goat anti-guinea pig IgG antibody and Alexa Fluor 488-conjugated goat anti-mouse IgG antibody, respectively. The immunostained tissues were observed by BZ9000 microscope (Keyence, Osaka, Japan).

Figure 5. Rescue Experiments of Insulin Secretion and the Number of Docked Insulin Granules in *Rim2α*$^{ko/ko}$ β Cells

(A) Effects of mutant Rim2α on insulin secretion and the number of insulin granules docked to the plasma membrane. (Upper-left) Glucose- and K^+-induced insulin secretion in *Rim2α*$^{ko/ko}$ β cells expressing mutant Rim2α. (Upper-left) The number of insulin granules docked to the plasma membrane in *Rim2α*$^{ko/ko}$ β cells expressing mutant Rim2α. In the absence of interaction of Rim2α and Rab3A, insulin granule exocytosis is rather enhanced because the interaction induces docking of insulin granules, which prevents fusion to the plasma membrane (braking) (lower-left). In contrast, mutant Rim2α that cannot bind to Munc13-1 but can bind to Rab3A allows the granules to dock. Because priming is not initiated in this state, fusion events do not occur (lower-right). *$p < 0.01$ versus corresponding values in Ad-β-gal (Dunnett's method). †$p < 0.01$ versus corresponding values in Ad-WT Rim2α (Tukey-Kramer method).

(B) Effect of PMA stimulation on insulin secretion (left) and the number of insulin granules docked to the plasma membrane (middle). (Right) Model for insulin granule exocytosis in *Rim2α*$^{ko/ko}$ β cells stimulated with PMA. *$p < 0.01$ versus corresponding values in the absence of PMA (Student's unpaired t test).

(C) Effect of Syntaxin1 on insulin secretion (left) and the number of insulin granules docked to the plasma membrane (middle). (Right) Model for insulin granule exocytosis in *Rim2α*$^{ko/ko}$ β cells expressing open Syntaxin1. *$p < 0.01$ versus corresponding values in Ad-β-gal (Dunnett's method).

Data were obtained from three independent experiments (n = 7–11) and expressed as means ± SEM. Red, Rim2α; blue, Rab3A; green, Munc13-1.

See also Figure S3.

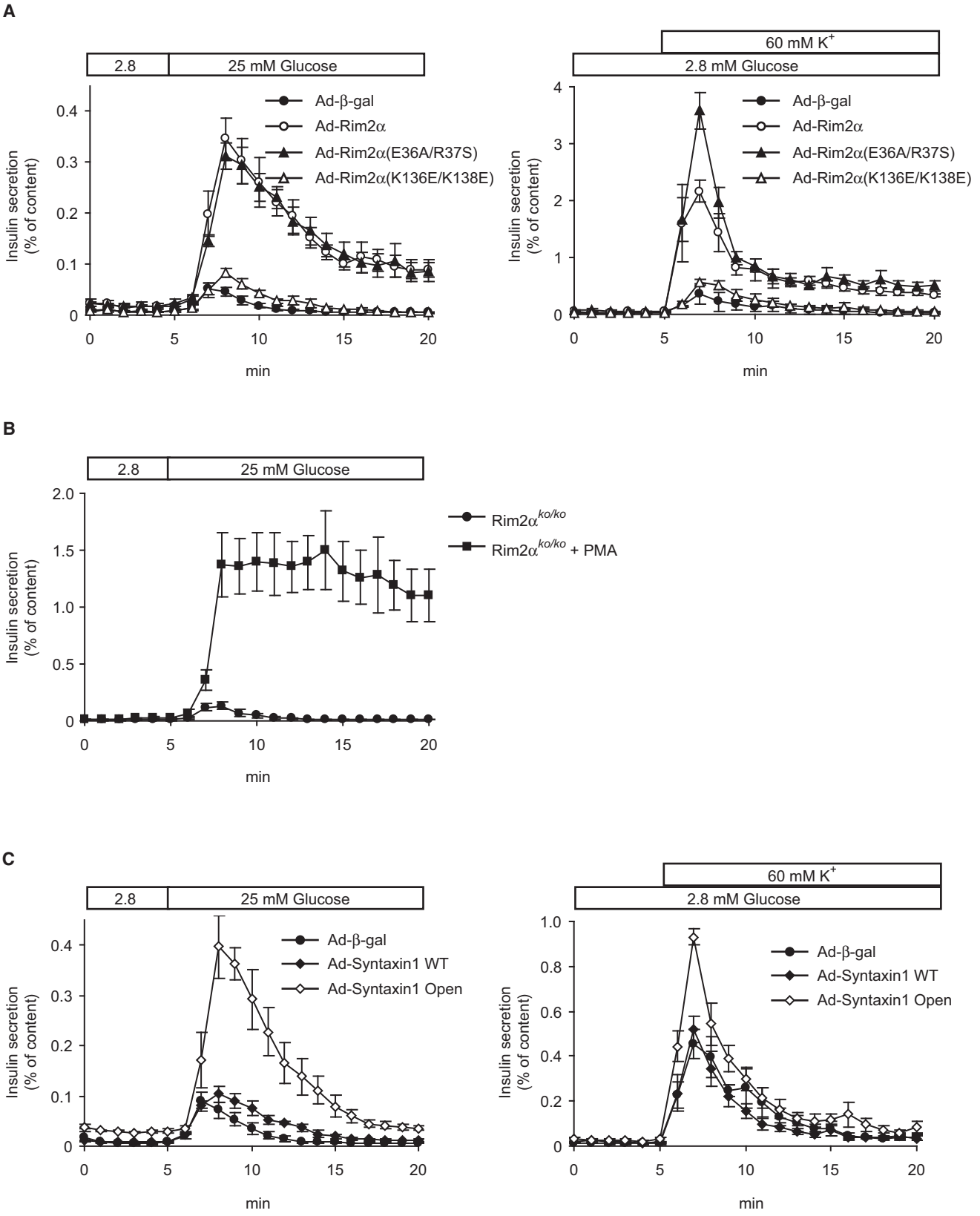
A
2.8
25 mM Glucose
Ad-β-gal
Ad-Rim2α
Ad-Rim2α(E36A/R37S)
Ad-Rim2α(K136E/K138E)
Insulin secretion (% of content)
min
60 mM K+
2.8 mM Glucose
B
Rim2α ko/ko
Rim2α ko/ko + PMA
C
Ad-Syntaxin1 WT
Ad-Syntaxin1 Open

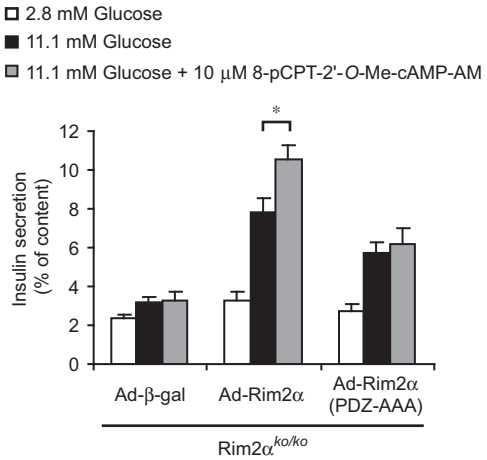

Figure 7. Effect of the Triple-Mutant Rim2α on Epac2-Mediated Exocytosis

Rim2α$^{ko/ko}$ β cells expressing Rim2α (PDZ-AAA) were stimulated with 11.1 mM glucose plus 10 μM 8-pCPT-2′-*O*-Me-cAMP-AM. Data were obtained from three independent experiments (n = 8–11) and expressed as means ± SEM. *p < 0.01 (Dunnett's method).

Immunocytochemical Analysis

MIN6 cells and *Rim2α*$^{ko/ko}$ β cells were fixed with 3.7% formaldehyde in 0.1 M phosphate buffer (pH 7.4) for 10 min at room temperature and thoroughly rinsed with 0.1 M PBS. After the samples were pretreated with 0.1% Triton X-100 and 10% normal goat serum, they were incubated with guinea pig anti-insulin antibody and rabbit anti-Rim2 antibody, followed by Alexa Fluor 546-conjugated goat anti-guinea pig IgG antibody and Alexa Fluor 488-conjugated goat anti-rabbit IgG antibody, respectively. The immunostained cells were observed by confocal laser scanning microscopy (FV1000; Olympus, Tokyo, Japan).

Insulin Secretion Experiments

Pancreatic islets were isolated from *Rim2α*$^{+/+}$ and *Rim2α*$^{-/-}$ mice by collagenase digestion and cultured for 2 days as described previously (Kashima et al., 2001). Thirty minutes after preincubation of isolated islets with HEPES-KRB buffer containing 2.8 mM glucose, five size-matched islets were collected in each well of a 96-well plate and incubated for 30 min in 100 μl of the same buffer containing various stimuli. Insulin released in the incubation buffer and cellular insulin content were measured by ELISA (Medical Biological Laboratories, Nagoya, Japan). The amount of insulin secretion was normalized by cellular insulin content. Insulin secretion experiments in MIN6 cells and *Rim2α*$^{ko/ko}$ β cells were performed as described above.

TIRFM Analysis

Primary cultured β cells isolated from mouse pancreatic islets were infected with adenovirus carrying insulin-Venus and subjected to analysis by TIRFM as previously described (Shibasaki et al., 2007). The number of granules docked to the plasma membrane was measured by G-Count software (G-Angstrom K.K, Miyagi, Japan).

Subcellular Fractionation

Discontinuous sucrose gradient fractionation of MIN6 cells and *Rim2α*$^{ko/ko}$ β cells were carried out as previously described (Sugawara et al., 2009).

Coimmunoprecipitation Experiments

Two days before coimmunoprecipitation experiments, COS-1 cells were transiently transfected with plasmids encoding FLAG-tagged Rab3A (Q81L) using Effectene Transfection Reagent (QIAGEN) according to the manufacturer's instruction. Coimmunoprecipitation experiments were performed using Pierce Mammalian c-Myc Tag IP/Co-IP Kit (Thermo Fisher Scientific, Waltham, MA) according to the manufacturer's instruction. In brief, *Rim2α*$^{ko/ko}$ β cells were infected with Ad-β-galactosidase (β-gal) or Ad-Rim2α. After 2 day culture, the infected cells were preincubated in HEPES-KRB buffer containing 2.8 mM glucose. Thirty minutes after preincubation, the cells were stimulated with HEPES-KRB buffer containing 2.8 mM glucose or 25 mM glucose for 30 min. The cells were then lysed in buffer containing 10 mM HEPES (pH 7.4), 150 mM NaCl, 0.5% CHAPS, 5 mM $MgCl_2$, and protease inhibitor cocktail and were collected in microcentrifuge tubes. The cellular lysates were incubated with 10 μl anti-c-Myc antibody conjugated with agarose in the absence or presence of cellular lysate of COS-1 transfected with FLAG-tagged Rab3A (Q81L). After incubation at 4°C for overnight, the agarose was washed five times with buffer containing 25 mM Tris-HCl, 150 mM NaCl, and 0.05% Tween 20 (pH 7.2), and the bound proteins were subjected to SDS-PAGE followed by immunoblot analysis with anti-Rim2, anti-Munc13, and anti-Rab3 antibodies.

Construction of Adenovirus Vectors

Rat Rab3A was subcloned into pFLAG-CMV-2 vector (Sigma). Site-directed mutagenesis of the N-terminal Zn^{2+}-finger domain (E36A/R37S and K136E/K138E mutants) and PDZ domain (PDZ-AAA mutant) in mouse Rim2α and L166A/E167A mutant in mouse Syntaxin1 was performed by the PCR-based method. Recombinant adenovirus carrying c-Myc-tagged WT Rim2α (Ad-Rim2α) or c-Myc-tagged mutants of Rim2α (Ad-Rim2α mutants) were generated according to the manufacturer's instruction (Stratagene, La Jolla, CA).

Perifusion Experiments

Perifusion experiments on insulin secretion of *Rim2α*$^{ko/ko}$ β cells were performed as described previously (Sugawara et al., 2009). In brief, the cells were seeded at a density of 5 × 10^5 cells on coverslips. The following day, the cells were infected with Ad-β-gal or Ad-Rim2α mutants or Ad-Syntaxin1 at an MOI of 1 and maintained for 48 hr. The cells were then incubated in HEPES-KRB containing 2.8 mM glucose for 50 min and mounted in a perifusion chamber. The cells were perifused in KRBH containing 2.8 mM glucose for 5 min, and the perfusate was then switched to HEPES-KRB containing 25 mM glucose or 60 mM K^+. Eluted fractions were collected at 1 min intervals, and released insulin in each fraction was measured by insulin assay kit (CIS bio international, Gif sur Yvette, France). The amount of secreted insulin was normalized by cellular insulin contents.

Statistical Analysis

The data are expressed as means ± SEM. Comparisons were made using Student's unpaired t test, Dunnet's method, or Tukey-Kramer's method as indicated in the legends. A probability level of $p < 0.05$ was considered statistically significant.

SUPPLEMENTAL INFORMATION

Supplemental Information includes Supplemental Experimental Procedures and four figures and can be found with this article online at doi:10.1016/j.cmet.2010.05.017.

Figure 6. Insulin Secretion from Perifused *Rim2α*$^{ko/ko}$ β Cells

(A) Effects of mutant Rim2α on insulin secretion. In the absence of interaction of Rim2α and Rab3A, K^+-induced insulin secretion is enhanced compared to that by WT Rim2α gene transfer. In contrast, mutant Rim2α that cannot bind to Munc13-1 does not restore either glucose- or K^+-induced insulin secretion.
(B) Effect of PMA stimulation on insulin secretion. Insulin secretion is induced by PMA even in the absence of Rim2α.
(C) Effect of Syntaxin1 on insulin secretion induced by glucose (left) and K^+ (right). Open Syntaxin1 rescues both glucose- and K^+-induced insulin secretion.
Data were obtained from two to three independent experiments (n = 4–5) and expressed as means ± SEM.
See also Figure S4.

ACKNOWLEDGMENTS

We thank G.K. Hokawa for assistance with the manuscript. This work was supported by a CREST grant from the Japan Science and Technology Agency and Grant-in-Aid for Scientific Research and by a grant for the Global Centers of Excellence Program "Global Center of Excellence for Education and Research on Signal Transduction Medicine in the Coming Generation" and "Global Center for Education and Research in Integrative Membrane Biology" from the Ministry of Education, Culture, Sports, Science and Technology.

Received: January 8, 2010
Revised: April 23, 2010
Accepted: May 26, 2010
Published: August 3, 2010

REFERENCES

Andrews-Zwilling, Y.S., Kawabe, H., Reim, K., Varoqueaux, F., and Brose, N. (2006). Binding to Rab3A-interacting molecule RIM regulates the presynaptic recruitment of Munc13-1 and ubMunc13-2. J. Biol. Chem. *281*, 19720–19731.

Ashery, U., Varoqueaux, F., Voets, T., Betz, A., Thakur, P., Koch, H., Neher, E., Brose, N., and Rettig, J. (2000). Munc13-1 acts as a priming factor for large dense-core vesicles in bovine chromaffin cells. EMBO J. *19*, 3586–3596.

Barg, S., Ma, X., Eliasson, L., Galvanovskis, J., Göpel, S.O., Obermüller, S., Platzer, J., Renström, E., Trus, M., Atlas, D., et al. (2001). Fast exocytosis with few Ca^{2+} channels in insulin-secreting mouse pancreatic B cells. Biophys. J. *81*, 3308–3323.

Betz, A., Ashery, U., Rickmann, M., Augustin, I., Neher, E., Südhof, T.C., Rettig, J., and Brose, N. (1998). Munc13-1 is a presynaptic phorbol ester receptor that enhances neurotransmitter release. Neuron *21*, 123–136.

Betz, A., Thakur, P., Junge, H.J., Ashery, U., Rhee, J.S., Scheuss, V., Rosenmund, C., Rettig, J., and Brose, N. (2001). Functional interaction of the active zone proteins Munc13-1 and RIM1 in synaptic vesicle priming. Neuron *30*, 183–196.

Brondyk, W.H., McKiernan, C.J., Burstein, E.S., and Macara, I.G. (1993). Mutants of Rab3A analogous to oncogenic Ras mutants. Sensitivity to Rab3A-GTPase activating protein and Rab3A-guanine nucleotide releasing factor. J. Biol. Chem. *268*, 9410–9415.

Brunner, Y., Couté, Y., Iezzi, M., Foti, M., Fukuda, M., Hochstrasser, D.F., Wollheim, C.B., and Sanchez, J.C. (2007). Proteomics analysis of insulin secretory granules. Mol. Cell. Proteomics *6*, 1007–1017.

Burgoyne, R.D., and Morgan, A. (2003). Secretory granule exocytosis. Physiol. Rev. *83*, 581–632.

Castillo, P.E., Schoch, S., Schmitz, F., Südhof, T.C., and Malenka, R.C. (2002). RIM1α is required for presynaptic long-term potentiation. Nature *415*, 327–330.

Drucker, D.J. (2006). The biology of incretin hormones. Cell Metab. *3*, 153–165.

Dulubova, I., Sugita, S., Hill, S., Hosaka, M., Fernandez, I., Südhof, T.C., and Rizo, J. (1999). A conformational switch in syntaxin during exocytosis: role of munc18. EMBO J. *18*, 4372–4382.

Dulubova, I., Lou, X., Lu, J., Huryeva, I., Alam, A., Schneggenburger, R., Südhof, T.C., and Rizo, J. (2005). A Munc13/RIM/Rab3 tripartite complex: from priming to plasticity? EMBO J. *24*, 2839–2850.

Fujimoto, K., Shibasaki, T., Yokoi, N., Kashima, Y., Matsumoto, M., Sasaki, T., Tajima, N., Iwanaga, T., and Seino, S. (2002). Piccolo, a Ca^{2+} sensor in pancreatic β-cells. Involvement of cAMP-GEFII•Rim2•Piccolo complex in cAMP-dependent exocytosis. J. Biol. Chem. *277*, 50497–50502.

Fukuda, M. (2003). Distinct Rab binding specificity of Rim1, Rim2, rabphilin, and Noc2. Identification of a critical determinant of Rab3A/Rab27A recognition by Rim2. J. Biol. Chem. *278*, 15373–15380.

Fukuda, M. (2004). Alternative splicing in the first α-helical region of the Rab-binding domain of Rim regulates Rab3A binding activity: is Rim a Rab3 effector protein during evolution? Genes Cells *9*, 831–842.

Fukui, K., Yang, Q., Cao, Y., Takahashi, N., Hatakeyama, H., Wang, H., Wada, J., Zhang, Y., Marselli, L., Nammo, T., et al. (2005). The HNF-1 target collectrin controls insulin exocytosis by SNARE complex formation. Cell Metab. *2*, 373–384.

Gomi, H., Mizutani, S., Kasai, K., Itohara, S., and Izumi, T. (2005). Granuphilin molecularly docks insulin granules to the fusion machinery. J. Cell Biol. *171*, 99–109.

Hibino, H., Pironkova, R., Onwumere, O., Vologodskaia, M., Hudspeth, A.J., and Lesage, F. (2002). RIM binding proteins (RBPs) couple Rab3-interacting molecules (RIMs) to voltage-gated Ca^{2+} channels. Neuron *34*, 411–423.

Hoppa, M.B., Collins, S., Ramracheya, R., Hodson, L., Amisten, S., Zhang, Q., Johnson, P., Ashcroft, F.M., and Rorsman, P. (2009). Chronic palmitate exposure inhibits insulin secretion by dissociation of Ca^{2+} channels from secretory granules. Cell Metab. *10*, 455–465.

Inoue, E., Deguchi-Tawarada, M., Takao-Rikitsu, E., Inoue, M., Kitajima, I., Ohtsuka, T., and Takai, Y. (2006). ELKS, a protein structurally related to the active zone protein CAST, is involved in Ca^{2+}-dependent exocytosis from PC12 cells. Genes Cells *11*, 659–672.

Kang, L., He, Z., Xu, P., Fan, J., Betz, A., Brose, N., and Xu, T. (2006). Munc13-1 is required for the sustained release of insulin from pancreatic β cells. Cell Metab. *3*, 463–468.

Kasai, K., Ohara-Imaizumi, M., Takahashi, N., Mizutani, S., Zhao, S., Kikuta, T., Kasai, H., Nagamatsu, S., Gomi, H., and Izumi, T. (2005). Rab27a mediates the tight docking of insulin granules onto the plasma membrane during glucose stimulation. J. Clin. Invest. *115*, 388–396.

Kashima, Y., Miki, T., Shibasaki, T., Ozaki, N., Miyazaki, M., Yano, H., and Seino, S. (2001). Critical role of cAMP-GEFII—Rim2 complex in incretin-potentiated insulin secretion. J. Biol. Chem. *276*, 46046–46053.

Kiyonaka, S., Wakamori, M., Miki, T., Uriu, Y., Nonaka, M., Bito, H., Beedle, A.M., Mori, E., Hara, Y., De Waard, M., et al. (2007). RIM1 confers sustained activity and neurotransmitter vesicle anchoring to presynaptic Ca^{2+} channels. Nat. Neurosci. *10*, 691–701.

Koushika, S.P., Richmond, J.E., Hadwiger, G., Weimer, R.M., Jorgensen, E.M., and Nonet, M.L. (2001). A post-docking role for active zone protein Rim. Nat. Neurosci. *4*, 997–1005.

Llinás, R., Sugimori, M., and Silver, R.B. (1992). Microdomains of high calcium concentration in a presynaptic terminal. Science *256*, 677–679.

Lonart, G., Schoch, S., Kaeser, P.S., Larkin, C.J., Südhof, T.C., and Linden, D.J. (2003). Phosphorylation of RIM1α by PKA triggers presynaptic long-term potentiation at cerebellar parallel fiber synapses. Cell *115*, 49–60.

Madison, J.M., Nurrish, S., and Kaplan, J.M. (2005). UNC-13 interaction with syntaxin is required for synaptic transmission. Curr. Biol. *15*, 2236–2242.

Matsumoto, M., Miki, T., Shibasaki, T., Kawaguchi, M., Shinozaki, H., Nio, J., Saraya, A., Koseki, H., Miyazaki, M., Iwanaga, T., and Seino, S. (2004). Noc2 is essential in normal regulation of exocytosis in endocrine and exocrine cells. Proc. Natl. Acad. Sci. USA *101*, 8313–8318.

Ménasché, G., Pastural, E., Feldmann, J., Certain, S., Ersoy, F., Dupuis, S., Wulffraat, N., Bianchi, D., Fischer, A., Le Deist, F., and de Saint Basile, G. (2000). Mutations in RAB27A cause Griscelli syndrome associated with haemophagocytic syndrome. Nat. Genet. *25*, 173–176.

Miki, T., Minami, K., Shinozaki, H., Matsumura, K., Saraya, A., Ikeda, H., Yamada, Y., Holst, J.J., and Seino, S. (2005). Distinct effects of glucose-dependent insulinotropic polypeptide and glucagon-like peptide-1 on insulin secretion and gut motility. Diabetes *54*, 1056–1063.

Miyazaki, J., Araki, K., Yamato, E., Ikegami, H., Asano, T., Shibasaki, Y., Oka, Y., and Yamamura, K. (1990). Establishment of a pancreatic β cell line that retains glucose-inducible insulin secretion: special reference to expression of glucose transporter isoforms. Endocrinology *127*, 126–132.

Nicolson, T.J., Bellomo, E.A., Wijesekara, N., Loder, M.K., Baldwin, J.M., Gyulkhandanyan, A.V., Koshkin, V., Tarasov, A.I., Carzaniga, R., Kronenberger, K., et al. (2009). Insulin storage and glucose homeostasis in mice null for the granule zinc transporter ZnT8 and studies of the type 2 diabetes-associated variants. Diabetes *58*, 2070–2083.

Ohara-Imaizumi, M., Ohtsuka, T., Matsushima, S., Akimoto, Y., Nishiwaki, C., Nakamichi, Y., Kikuta, T., Nagai, S., Kawakami, H., Watanabe, T., and Nagamatsu, S. (2005). ELKS, a protein structurally related to the active

zone-associated protein CAST, is expressed in pancreatic β cells and functions in insulin exocytosis: interaction of ELKS with exocytotic machinery analyzed by total internal reflection fluorescence microscopy. Mol. Biol. Cell *16*, 3289–3300.

Ozaki, N., Shibasaki, T., Kashima, Y., Miki, T., Takahashi, K., Ueno, H., Sunaga, Y., Yano, H., Matsuura, Y., Iwanaga, T., et al. (2000). cAMP-GEFII is a direct target of cAMP in regulated exocytosis. Nat. Cell Biol. *2*, 805–811.

Richmond, J.E., Weimer, R.M., and Jorgensen, E.M. (2001). An open form of syntaxin bypasses the requirement for UNC-13 in vesicle priming. Nature *412*, 338–341.

Schoch, S., Castillo, P.E., Jo, T., Mukherjee, K., Geppert, M., Wang, Y., Schmitz, F., Malenka, R.C., and Südhof, T.C. (2002). RIM1α forms a protein scaffold for regulating neurotransmitter release at the active zone. Nature *415*, 321–326.

Schoch, S., Mittelstaedt, T., Kaeser, P.S., Padgett, D., Feldmann, N., Chevaleyre, V., Castillo, P.E., Hammer, R.E., Han, W., Schmitz, F., et al. (2006). Redundant functions of RIM1α and RIM2α in Ca^{2+}-triggered neurotransmitter release. EMBO J. *25*, 5852–5863.

Seino, S., and Shibasaki, T. (2005). PKA-dependent and PKA-independent pathways for cAMP-regulated exocytosis. Physiol. Rev. *85*, 1303–1342.

Seino, S., Takahashi, H., Fujimoto, W., and Shibasaki, T. (2009). Roles of cAMP signalling in insulin granule exocytosis. Diabetes Obes. Metab. *11* (*Suppl 4*), 180–188.

Shibasaki, T., Sunaga, Y., Fujimoto, K., Kashima, Y., and Seino, S. (2004). Interaction of ATP sensor, cAMP sensor, Ca^{2+} sensor, and voltage-dependent Ca^{2+} channel in insulin granule exocytosis. J. Biol. Chem. *279*, 7956–7961.

Shibasaki, T., Takahashi, H., Miki, T., Sunaga, Y., Matsumura, K., Yamanaka, M., Zhang, C., Tamamoto, A., Satoh, T., Miyazaki, J., and Seino, S. (2007). Essential role of Epac2/Rap1 signaling in regulation of insulin granule dynamics by cAMP. Proc. Natl. Acad. Sci. USA *104*, 19333–19338.

Sudhof, T.C. (2004). The synaptic vesicle cycle. Annu. Rev. Neurosci. *27*, 509–547.

Sugawara, K., Shibasaki, T., Mizoguchi, A., Saito, T., and Seino, S. (2009). Rab11 and its effector Rip11 participate in regulation of insulin granule exocytosis. Genes Cells *14*, 445–456.

Verhage, M., and Sørensen, J.B. (2008). Vesicle docking in regulated exocytosis. Traffic *9*, 1414–1424.

Vliem, M.J., Ponsioen, B., Schwede, F., Pannekoek, W.J., Riedl, J., Kooistra, M.R., Jalink, K., Genieser, H.G., Bos, J.L., and Rehmann, H. (2008). 8-pCPT-2′-*O*-Me-cAMP-AM: an improved Epac-selective cAMP analogue. ChemBioChem *9*, 2052–2054.

Wang, Y., and Südhof, T.C. (2003). Genomic definition of RIM proteins: evolutionary amplification of a family of synaptic regulatory proteins(small star, filled). Genomics *81*, 126–137.

Wang, Y., Okamoto, M., Schmitz, F., Hofmann, K., and Südhof, T.C. (1997). Rim is a putative Rab3 effector in regulating synaptic-vesicle fusion. Nature *388*, 593–598.